Desalination and Water Treatment
www.deswater.com

doi: 10.5004/dwt.2019.23536

147 (2019) 90–98
April

Aerobic granular sludge in a sequencing batch reactor for tomato paste processing wastewater treatment: formation, characteristics, and microbial community structure

Weihong Wang[a,*], Yanshan Wang[a], Xinliao Dong[a], Qianqian Liu[a], Qiwei Chen[b]

[a]*College of Hydraulic and Civil Engineering, Xinjiang Agricultural University, Urumqi 830052, China, Tel. +86 13899910629; email: 2209319288@qq.com (W. Wang), Tel. +86 18699490636; email: 1009320495@qq.com (Y. Wang), Tel. +86 18899192157; email: 595929202@qq.com (X. Dong), Tel. +86 13039454827; email: 837543519@qq.com (Q. Liu)*
[b]*Department of Civil Engineering, Hefei University of Technology, Hefei 230009, China, Tel. +86 15755166922; email: cqw930721@163.com (Q. Chen)*

Received 23 May 2018; Accepted 27 November 2018

ABSTRACT

In this study, a dense and stable aerobic granular sludge with excellent settling properties (with sludge volume index after 5 min of settling (SVI_5) decreased to 19.46 mL/g and SVI_{30}/SVI_5 = 1) and diameter size of approximately 10 mm was successfully cultivated in a sequencing batch reactor system fed with synthetic tomato paste to process wastewater. Concurrently, average removal rate of chemical oxygen demand of 95.53% was achieved at different organic loads in the system during the operation for 185 d. The combination of the bioanalytical techniques of confocal laser scanning microscopy, live/dead staining, and high-throughput sequencing were used to characterize the granulation process of activated sludge. The results showed that protein and α-D-glucopyranose polysaccharide were widely distributed throughout the granules and formed a framework of the granules. The pores in the granules provided the pathways for the nutrients and dissolved oxygen transport, and thus, live bacteria were located outside of the granule and around the internal pores. The community diversity and richness varied during the sludge granulation process. The dominant degradation bacteria at class level were shifted from the *Betaproteobacteria* and *Alphaproteobacteria* to *Gammaproteobacteria* and *Betaproteobacteria* after the granule sludge was formed. The succession of microbial communities showed cooperative effects of different bacterial communities, which may play a significant role in the degradation of tomato paste processing wastewater and stability of the system.

Keywords: Tomato paste processing wastewater; Aerobic granular sludge; Organic loads; Extracellular polymeric substances (EPS); High-throughput sequencing

1. Introduction

Tomato production is one of the main agricultural food processing industry sectors, which plays an important role in the economy of Xinjiang, China. Presently, Xinjiang, whose annual export volume of tomato paste accounts for approximately 30% of the global trade volume of tomato paste, is one of the three major tomato- producing areas in the world [1]. However, the thriving tomato paste processing industry has resulted in a significant environmental issue—for each ton of tomato paste produced, 15–50 m^3 of wastewater is discharged with chemical oxygen demand (COD) in the range from 400 to 2,000 mg/L during processing, which should not be disregarded [2,3]. Tomato paste processing wastewater is characterized by high organic sugars and organic acids with an offensive smell, for which the most common treatment is a combined activated sludge process and physicochemical process [2,4,5]. However, owing to the seasonal nature of tomato paste processing wastewater production in Xinjiang (the tomato harvesting takes 60–90 d/y), the treatment

* Corresponding author.

effect is not ensured unless the well-performing sludge is re-domesticated and aggregated by using a strong microorganism in a short period each year.

Compared with conventional activated sludge systems, aerobic granules have unique superiority. For instance, they have high biomass retention, excellent settling properties, and anti-shock loading capability [6,7], and they have been broadly developed to treat different types of wastewater. However, to date, treatment of tomato processing wastewater with this technology has been scarcely reported.

Indeed, several studies have shown that aerobic granule technology is reasonable for the treatment of food processing industry wastewater. For example, Corsino et al. [8] reported that when using this technology to treat the wastewater produced by fish-canning processing industries, the COD and biochemical oxygen demand removal efficiencies were over 90% and more than 95% of the particulate organic matter was removed. Dobbeleers et al. [9] cultivated aerobic nitrite granules from potato industrial wastewater feed and achieved simultaneous nitrification/denitrification. Lilmaz et al. [10] found that the removal efficiencies of soluble COD, soluble phosphorus, and soluble nitrogen were 85%, 89%, and 93%, respectively, by using a granular sludge in the treatment of meat processing industry wastewater. Su et al. [11] used aerobic granules to treat the soybean processing wastewater in a sequencing batch reactor (SBR), and the results showed that the loading rate was increased from 1.5 to 6.0 kg COD/(m^3 d), and the COD removal efficiency was maintained between 98%% and 99%. Therefore, there is reason to believe that aerobic granular sludge could be feasible for its application in the treatment of tomato processing wastewater.

Nevertheless, the granulation process is still the key factor affecting the practical engineering application of an aerobic granular sludge. If the granular process could be systematically described, it would become possible to provide a scientific basis for accelerating the start-up process of the aerobic granular sludge system and further solve the problem of the short seasonal production cycle of tomato wastewater and long microbial start-up period.

Therefore, this study investigates the development of aerobic granules starting from a flocculent sludge during the treatment of tomato processing wastewater as well as the organic and nutrient removal performance. More precisely, confocal laser scanning microscope (CLSM) and high-throughput sequencing techniques are used to characterize the granular features of the granulation process. This can be useful for further understanding the aerobic granulation mechanism and optimizing the operating conditions for the treatment of tomato processing wastewater.

2. Materials and methods

2.1. Reactor setup and operational strategies

The schematic of the laboratory-scale reactor is presented in Fig. 1. An SBR with a working volume of 4 L and height (1 m) to internal diameter (0.08 m) ratio (*H*/*D*) of 12.5 was used for the cultivation of aerobic granules. Furthermore, the SBR reactor was automatically controlled with a time controller (Influent pump (Lead Fluid, China), Aeration pump (SunSun Incorporated, China), Effluent valve

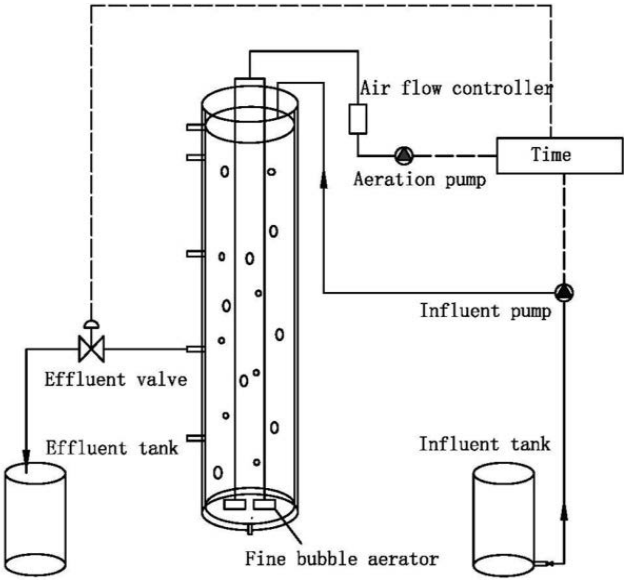

Fig. 1. SBR schematic.

(Fangwei Incorporated, China), Air flow controller (Dongxing Incorporated, China), and Time controller (Kerde, China)). The reactor was operated with cycles of 4 h, including 10 min of feeding, 198–227.5 min of aeration, 0.5–30 min of settling, and 2 min of effluent discharging. The hydraulic retention time (HRT) was 8 h, and volumetric exchange ratio was 50%.

During the experiment, the SBR operation of 185 d was divided into six periods characterized by increasing the influent COD concentrations from 400 to 2,000 mg/L gradually; correspondingly, the organic load was increased from 1.25 to 6 kg COD/(m^3 d). The specific operating parameters are listed in Table 1.

2.2. Seed sludge

Conventional activated sludge (1.5 L) taken from an aeration tank of a tomato processing wastewater treatment plant in Xinjiang, China, was used as the seed with mixed liquor suspended solids (MLSS) of 5.61 g/L and sludge volume index after 5 min of settling (SVI_5) of 146.3 mL/g.

2.3. Synthetic tomato paste processing wastewater

The synthetic tomato paste processing wastewater used as the feed solution was made by squeezing fresh tomato juice as the sole carbon source and adding NH_4CL and Na_2HPO_4 as the nitrogen and phosphorus sources, respectively. The characteristics of the synthetic wastewater are listed in Table 1. The composition of the microelement solution was based on the results of previous reports [12]. The pH was adjusted to 7.5–8.5 using Na_2CO_3.

2.4. Analytical methods

2.4.1. Conventional index analysis

The SVI_5, SVI_{30}, MLSS, mixed liquor volatile suspended solids (MLVSS), and COD were measured according to

Table 1
Operation parameters and synthetic influent characteristics of the SBR

Parameter/component	Stage I	Stage II	Stage III	Stage IV	Stage V	Stage VI
Operating day	1–22	23–65	67–123	124–143	144–167	168–185
Influent feeding (min)	10	10	10	10	10	10
Aeration (min)	198–201	211–223	223–227	227	227.5	227.5
Settling (min)	30–17	17–5	5–1	1	0.5	0.5
Effluent discharging (min)	2	2	2	2	2	2
COD (mg/L)	400 ± 18	800 ± 24	1,300 ± 23	1,700 ± 28	2,000 ± 26	1,400 ± 22
NH_4^+–N (mg/L)	55.47	58.49	67.4	66.45	61.11	51.53
PO_4^{3-}–P (mg/L)	10 ± 2.5	10 ± 2.5	10 ± 2.5	10 ± 2.5	10 ± 2.5	10 ± 2.5
pH	7.5–8.5	7.5–8.5	7.5–8.5	7.5–8.5	7.5–8.5	7.5–8.5
OLR (kg COD/(m^3 d))	1.25	2.47	3.98	5.02	6	4.13
HRT (h)	8	8	8	8	8	8

standard methods [13]. The morphology of the sludge during the granulation stages was observed via digital microscopy (Motic, China), a digital camera (Nikon, Japan), and stereomicroscope (ZEISS, Germany). The granular sludge size distribution was measured by the sieving method [14], and four different sieves with the opening sizes of 0.45, 1, 1.6, and 2 mm were used.

2.4.2. Extracellular polymeric substance staining and CLSM image analysis

The localization and distribution of extracellular polymeric substances (EPS) were observed via fluorescent staining coupled with CLSM. In this study, fluorescein isothiocyanate (FITC), concanavalin A (Con A), calcofluor white, and SYTO 63 (a cell-permeative nucleic acid stain) were used as fluorescent probes to stain proteins, α-polysaccharides, β-polysaccharides, and the total cells, respectively. The staining method as described previously [15,16] was used. The detailed procedure was as follows: A freshly sampled granule was washed thrice with phosphate-buffered saline (PBS) buffer and then stained with SYTO 63 (20 μM), FITC (10 g/L), Con A (0.25 g/L), and finally with calcofluor white (0.3 g/L) sequentially for 30 min each. After each staining, the sample was washed with PBS buffer thrice to remove the excess staining solution. The stained granular sludge was embedded for cryosectioning and frozen at −20°C. Subsequently, a 60 -μm section was cut on a cryogenic microtome and mounted on the CSLM (CLSM, ZEISS LSM710, Germany) slides for observation. The microscopic images were analyzed using ZEN 2009 software (ZEISS).

2.4.3. Live/dead bacteria staining

In this experiment, the staining of the live/dead bacteria in aerobic granular sludge was based on previous studies [17,18]. LIVE/DEAD BacLight Bacterial Viability Kit, L-7012, a fluorescent bacterial stain, contains two components: propidium iodide (PI, 20 mM) and SYTO 9 (3.34 mM). During staining, first PI (2 μL) and SYTO 9 (2 μL) were mixed evenly and then 400 μL of deionized water was added to dilute the stain. Subsequently, the aerobic granular sludge removed from the SBR reactor was washed thrice with PBS buffer and then placed in a well-diluted staining solution for 2 h. Then, the stained granular sludge was taken out and washed thrice with PBS buffer to remove the excess staining solution. Next, the granular sludge was embedded in an optimal cutting temperature compound embedding agent and frozen at −20°C to be sectioned into 60-μm sections in a cryomicrotome (Leica, Germany). Finally, the observations were made by a fluorescence microscope (Olympus, Japan), and the images were obtained by Cellsens software (Olympus, Japan).

2.4.4. Microbial diversity and community succession analysis during granulation

In this study, high-throughput sequencing techniques offered powerful tools to obtain a deeper insight into the microbial diversity and community succession in the process of degrading the synthesized tomato processing wastewater with granule formation. Four representative sludge samples were taken from different periods of 1, 15, 35, and 60 d and numbered as *W*1, *W*2, *W*3, and *W*4, respectively. The sludge–water mixture in each sample was packaged in sterile 50-mL centrifuge tubes and stored at −10°C. Deoxyribonucleic acid (DNA) extraction and polymerase chain reaction primer synthesis were completed by Sangon Biotech (Shanghai, China) Co., Ltd. Genomic DNA of the four sludge samples was extracted using the E.Z.N.ATM Mag-Bind Soil DNA Kit (OMEGA, USA), and the extracted DNA was amplified by using universal primers of V3–V4 region of 16 S recombinant DNA with 341 F primer (CCTACACGACGCTCTTCCGA TCTNCCTACGGGNGGCWGCAG) and 805 R primer (GACTGGAGTTCCTTGGCACCCGAGAATTCCAGACTAC HVGGGTATCTAATCC).

3. Results and discussion

3.1. Variation in physical characteristics of sludge during granulation

The sludge morphology is shown in Fig. 2. The inoculation flocculent sludge structure is loose and brown and the equivalent diameter of the sludge area is approximately

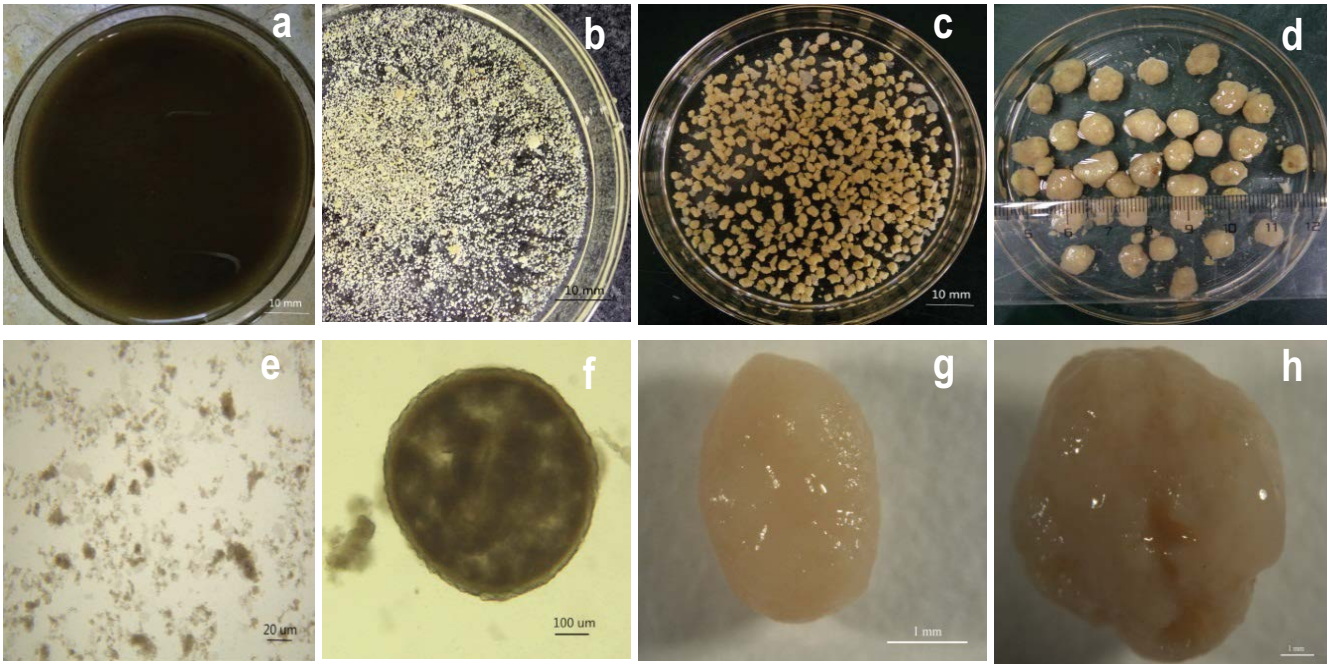

Fig. 2. Images of sludge morphology during different periods: (a) seed sludge, (b) granular sludge at 38 d of operation, (c) granular sludge at 90 d of operation, (d) granular sludge at 185 d of operation, (e, f) the microscopic image corresponding to (a) and (b) periods, respectively, and (g, h) the stereomicroscopic images corresponding to (a) and (b) periods, respectively.

15 μm, as shown in Figs. 2(a) and (e). After 38 d, the flocculent sludge gradually tends to yellow millet granules with the diameter increasing to 502 μm and structure becoming dense (Figs. 2(b) and (f)). To constantly reduce the settling time, more slow settling sludge was washed out from the reactor, leading to the accumulation of the aerobic granules with a high settling velocity. As shown in Figs. 2(c) and (g), after 90 d, the granules change to a more regular shape with the diameter increased to approximately 2 mm. A clear outline, compact structure, and smooth surface are observed clearly by the stereomicroscope. After 185 d, the granules reach a diameter of 10 mm with an average of approximately 5 mm, where some of the granules appear hollow on the surface (Figs. 2(d) and (h)). The surface hollowness may be related to the apoptosis of the bacteria, and its existence provides the pathway for internal material transport. In this study, the granule size of the culture was significantly higher than in the previous studies [19–21]. This might be owing to the synthetic wastewater and twisting of the long filament structures occurring in the larger granules, which is similar to that observed by Moghaddam et al. [22], who cultivated granules as large as 16 mm during a purely aerobic SBR operation.

From Fig. 3, it is clear that the particle size gradually increases during the entire time of operation. The average particle size of the inoculated sludge is below 20 μm. After 40 d of adaptation, although there are no granules formed with a size above 2 mm, the size of the granules based on the weight percentage is mainly concentrated in the range of 0.45–1 mm, accounting for nearly 52.5%. After 180 d, the granule diameter of 1.6–2 mm and above 2 mm increases from 3% and 0% to 19% and 57%, respectively, and eventually attains an advantageous range.

The physical characteristics of the sludge in terms of MLSS, MLVSS, and SVI are presented in Fig. 4. One week after inoculation, the MLSS decreases from 5.61 to 3.2 g/L owing to the reduction in the settling time and exclusion of the sludge with low settleability from the reactor. This is followed by a gradual increase in the MLSS to 12.5 g/L at 68 d. It can be concluded that the microbes grow rapidly under suitable environmental conditions. Concurrently, MLVSS/MLSS increases from 42.78% to 95.45%, indicating that the biological activity gradually increases with the reactor operation. As the organic loading rate (OLR) increases, MLSS reaches 11.3 g/L on day 142nd ay. Therefore, sludge discharge is performed until MLSS drops to 4.5 g/L. Based on the SVI_5

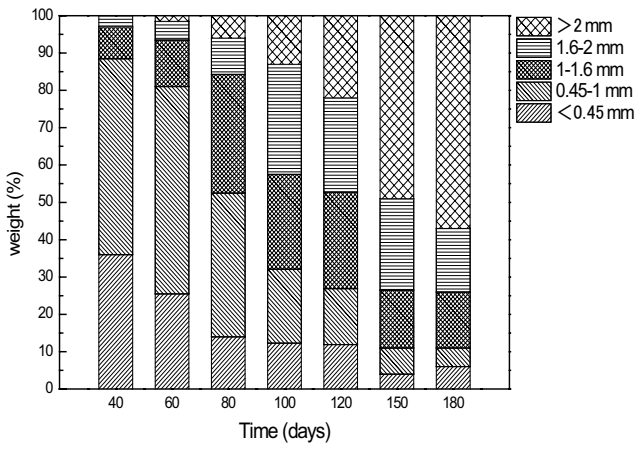

Fig. 3. Particle size distribution of the granules.

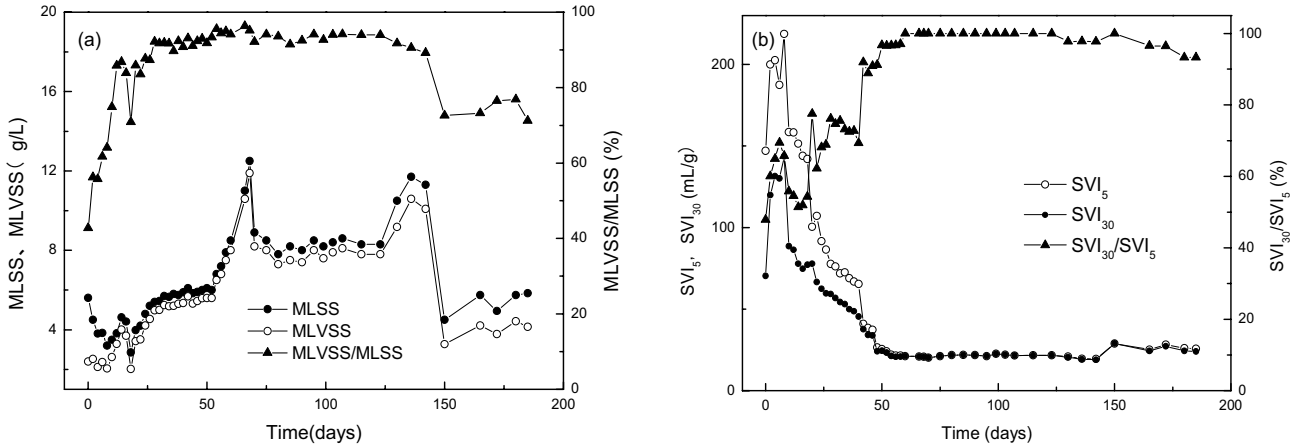

Fig. 4. Variation in the SVI, MLSS, and MLVSS in the SBR during the granulation process: (a) MLSS, MLVSS, and MLVSS/MLSS and (b) SVI_5, SVI_{30}, and SVI_{30}/SVI_5.

analyses, the low settling floc concentration decreases from 200 mL/g on day 2 to 65 mL/g on day 40 and to 19.46 mL/g on day 142. The ratio values of SVI_{30}/SVI_5 is 100%. This result is quite similar to that of Caluwé [23], where the reactor reached an SVI_{30}/SVI_{10} ratio equal to 1 during the treatment of petrochemical wastewater. This implies that an excellent settleability is obtained with the granule formation in the treatment of the synthetic tomato processing wastewater.

3.2. Organics and nutrient removal efficiency during granulation

The result of the SBR effluent quality in terms of the COD concentration is exhibited in Fig. 5. In this study, during the first stage, when the influent COD is 400 mg/L at 1.25 kg COD/(m^3 d), the COD in the effluent is not stable, with a maximum of 138 mg/L. During the II–IV stages of operation, the COD concentrations in the influent of the reactor is increased from 800 to 1,700 mg/L with a corresponding OLR increase from 2.47 to 5.02 kg COD/(m^3 d); correspondingly, the removal efficiency is improved to 97.7% and average removal efficiency of 95.53% is achieved. This efficiency is higher than that reported by Wang et al. [24], who in the treatment of industrial effluents applied OLR ranging between 0.7 and 5 g COD/(L d) to obtain removal efficiencies of 60%–95%. In our work, as the COD is increased to 2,000 mg/L with a corresponding OLR increase to 6 kg COD/(m^3 d), the removal efficiency begins to decline. Subsequently, even if the COD is reduced to 1,400 mg/L, the removal efficiency did not improve and average removal rate was maintained at 90.18%. This could be owing to the excessive sludge discharge on day 150 of the reaction which resulted in a significant decrease in the MLSS from 9.3 to 4.5 g/L, causing a loss of a numerous dominant bacteria. However, in general, the organic substrates in the synthetic tomato processing wastewater can be removed successfully.

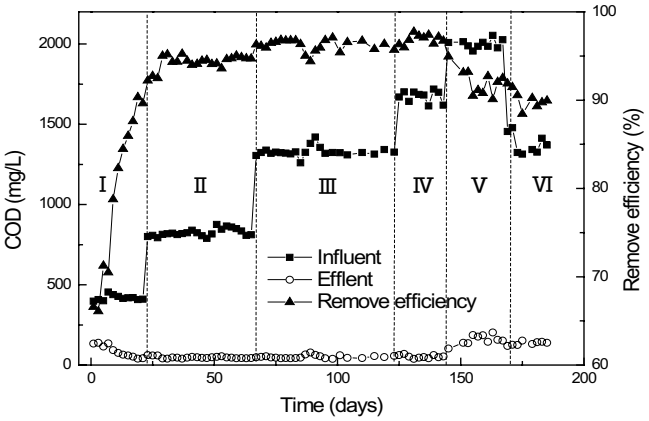

Fig. 5. Evaluation of different concentrations of COD in SBR process.

3.3. Distribution of stained EPS in granule

Figs. 6(a)–(f) presented the appearance of the outer surface and fluorescent staining results from the 65th day of tomato juice-fed granules. In this study, β-D-glucopyranose polysaccharides are mainly distributed on the outer edge of the granules (Fig. 6(c)). The protein and α-D-glucopyranose polysaccharide are widely distributed throughout the granules, which are the main components of granules and constitute the skeleton of the granules (Figs. 6(d)–(f)). The cells accumulate primarily on the outer region of the granules (Fig. 6(f)). These results are not in agreement with those of Chen et al. [15] and Adav et al. [25]. The former reported that β-D-polysaccharide was distributed throughout the interior of their acetate-fed granules and α-D-glucopyranose polysaccharide accumulated in the outer layer. The latter considered that β-D-polysaccharide was distributed both inside and outside of their phenol-fed granules. It is possible that the differences in the distribution of EPS owe to the different wastewater feed and operating conditions under which the granules are developed.

3.4. Distribution of live and dead bacteria in granules

The staining data of the particles according to the 65th day are presented in Figs. 7(a)–(c), the granular sludge cultured with the tomato juice feed has fewer live bacteria (green) in

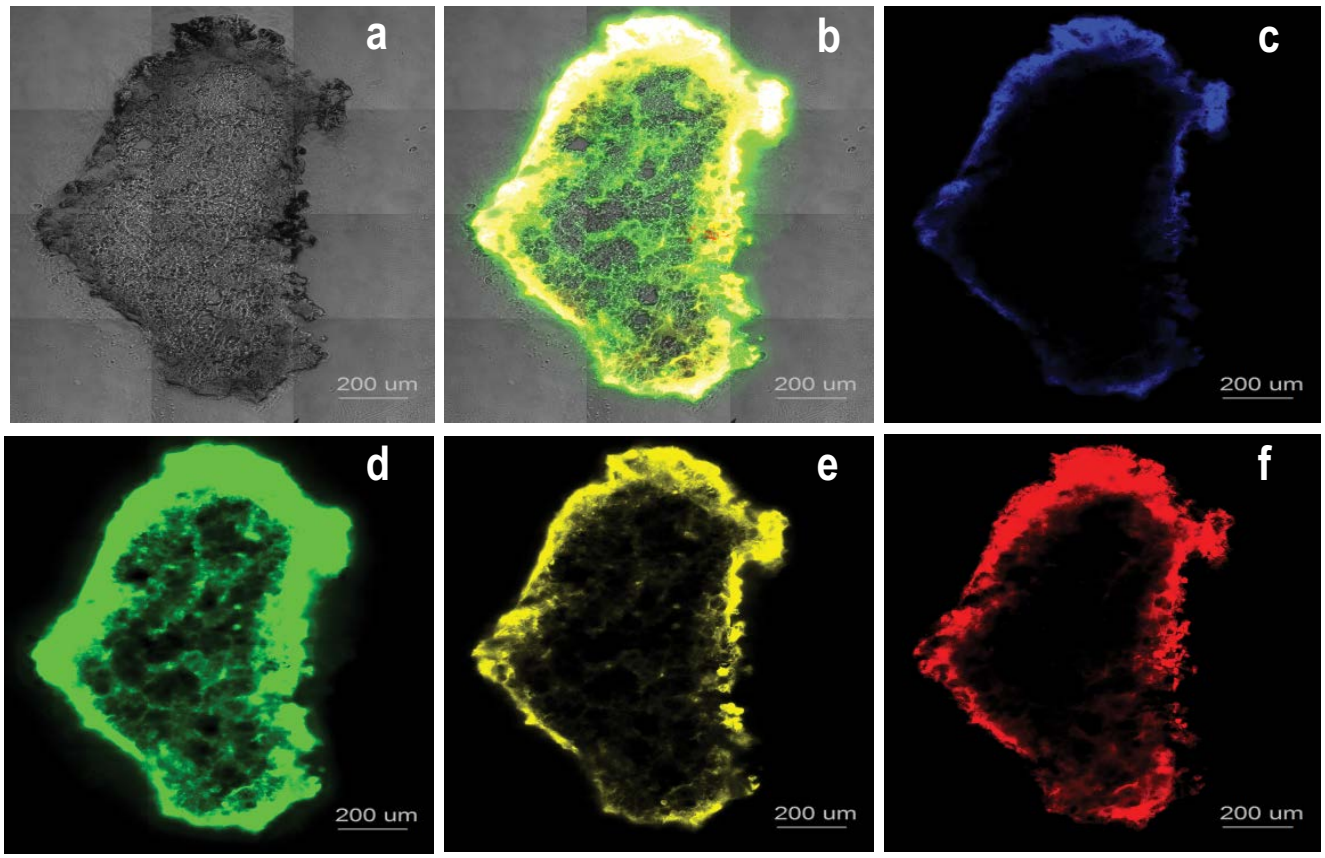

Fig. 6. CLSM images of the aerobic granules: (a) phase contrast photograph, (b) combined images of (c)–(f), (c) CLSM image of β-D-glucopyranose polysaccharides (calcofluor white), (d) CLSM image of protein (FITC), (e) CLSM image of α-D-glucopyranose polysaccharides (Con A), and (f) CLSM image of the cells (SYTO 63).

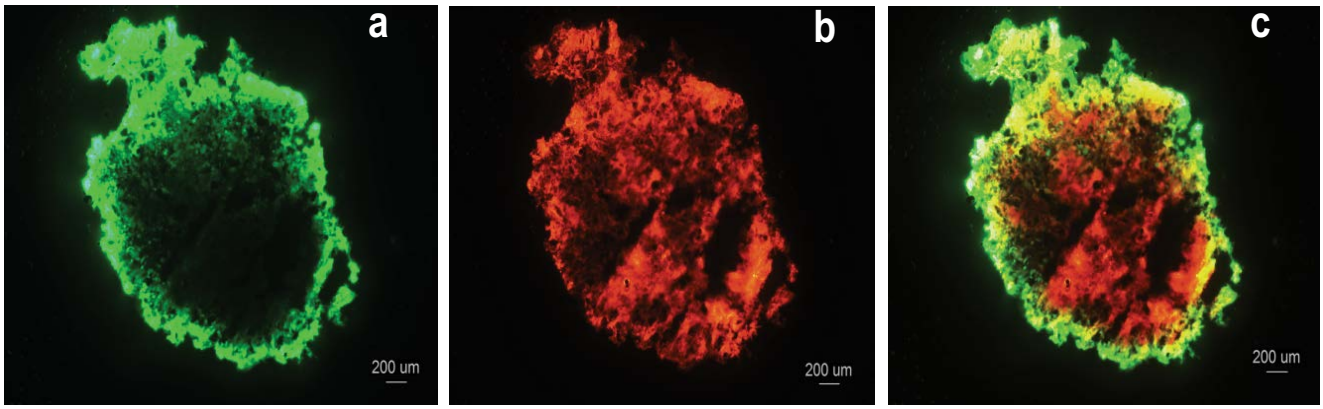

Fig. 7. Live and dead images of aerobic granules: (a) live bacteria, (b) dead bacteria, and (c) combined image of (a) and (b).

the granular cross section than the dead bacteria (red). The dead bacteria are located relative to the granule interior, whereas the live bacteria are more concentrated on the outer region of the granules and around the internal pores, which is similar to previous reports [25,26]. This is primarily because the granule size gradually increases and the mass transfer limitations cause the death of the bacteria in the interior of the granules, whereas on the outer layer, the delivery of the dissolved oxygen and nutrients sustains the growth of the microorganisms.

3.5. Microbial diversity and community succession analysis during granule formation

As can be seen from Table 2, the high-throughput sequencing yields 63,228, 58,968, 72,102, and 71,276 high-quality reads

Table 2
Community richness and diversity indices inferred by the microbial community

Sample ID	Sequence number	OTU number	Shannon index	ACE index	Chao1 index	Coverage
*W*1	63,288	4,408	4.69	88,850.37	32,467.74	0.94
*W*2	58,968	3,499	4.16	103,576.57	33,271.78	0.95
*W*3	72,102	4,087	3.67	119,758.64	40,066.93	0.95
*W*4	71,276	3,982	3.85	121,611.41	41,595.51	0.95

after filtering the low-quality and irrelevant sequences for samples *W*1–*W*4, respectively, all with >94% coverage. The community richness index of Chao 1 and ACE reveals the same trend. The sequence of the richness indices in *W*1–*W*4 is *W*4 > *W*3 > *W*2 > *W*1. The results verify that the inoculated sludge has a low richness and that the microbial community richness of the granules gradually increases during the sludge granulation process. Shannon indices of the community range from 3.67 to 4.69, showing an alpha diversity higher than that of numerous industrial wastewater types, such as acrylic polymer wastewater, textile dyeing wastewater, and petroleum refinery but lower than that of municipal wastewater [27].

Fig. 8 displays that in *W*1–*W*4 communities, the number of bacterial phylum is 15, 12, 11, and 12, respectively, giving a total of 19 phyla. The diversity of the bacteria first decreases and then increases in the four samples. The community structure in *W*1 is even more diversified than in the other samples. Such changes could be related to the shortening of the sludge settling time, resulting in a poor settling performance of the sludge excluded from the reactor and significant decrease in the sludge concentration which decrease the bacterial diversity. In addition, the OLR is increased from 1.25 to 2.47 kg COD/(m^3 d) on day 22, which also has a significant impact on the species selection during the aerobic granulation; similar conclusion was reported by Li et al. [28].

The *Proteobacteria*, *Bacteroidetes*, and *Firmicutes* phyla were the predominant bacteria in all the samples and could adapt best in response to the changes in the external environment. *Proteobacteria* is also reported as the prominent phylum in various bio-treatment systems such as coking wastewater, pet food industrial wastewater, and pharmaceutical and petroleum refinery wastewater treatment systems

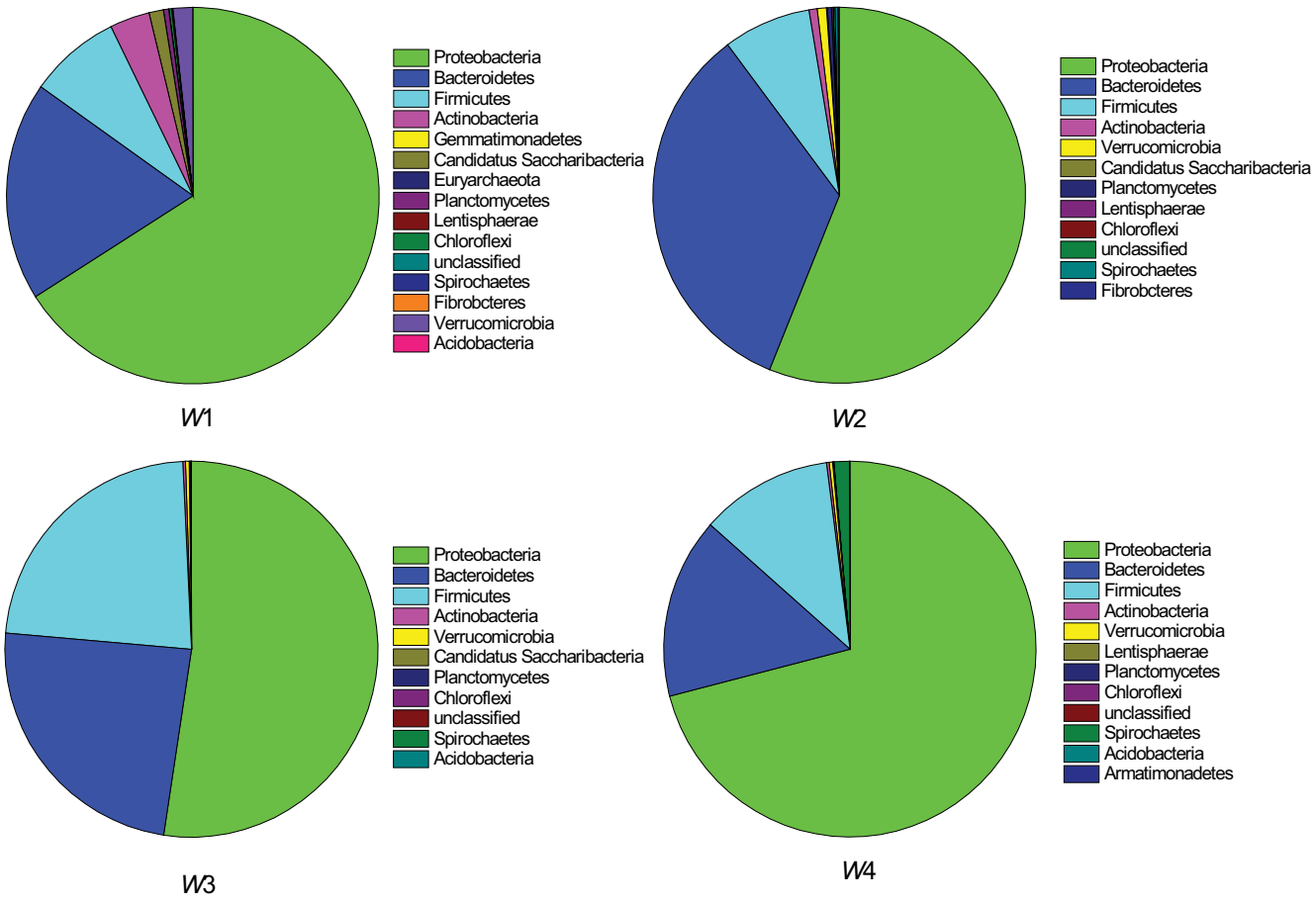

Fig. 8. Phyla classification level distribution of the bacteria from different periods.

[27,29] owing to the rich strains as well as the diversity of the metabolic pathways. With the granulation process, new types of microbial communities emerge in sample *W*4, such as *Armatimonadetes* and *Acidobacteria*.

Conversely, the initial proportion of *Proteobacteria* and *Firmicutes* is 66% and 7.95%, respectively, which increase to 70.93% and 11.48% in sample *W*4, respectively. According to the reports by Sun et al. [30] and Cao et al. [31], tomato processing wastewater degrades by screening with a strain of seven high-efficient dominant microorganisms, of which *Bacillus cereus* belongs to *Firmicutes* and *Pseudomonas putida* and *Pantoea agglomerans* belong to *Proteobacteria*. We can conclude that *Proteobacteria* and *Firmicutes* play a crucial role in the efficient degradation of tomato paste processing wastewater. In addition, compared with other competitive bacteria, *Firmicutes* can better protect themselves from the impact of the organic load owing to their thick cytoderm. Therefore, the abundance of *Firmicutes* increases with the influent COD enhancement to 800 from 400 mg L^{-1}. From the above, it can be deduced that the change in the number and type of microbial communities in samples *W*1–*W*4 facilitates the formation of aerobic granules and causes the degradation of the tomato processing wastewater.

The distribution of the microbial class classification levels in the different periods is shown in Fig. 9. The results exhibit more significant differences in the bacterial community structure in the samples at the class classification level than the phylum. In sample *W*1, *Alphaproteobacteria* and *Betaproteobacteria*, two classes of *Proteobacteria*, account for 14.5% and 42.99% of the sequences, respectively, attaining a predominant position in the total microbial profile. *Clostridia*, a class of *Firmicutes*, only accounts for 4.27%. In sample *W*2, the number of sequences of *Betaproteobacteria* decreases to 25.55%, whereas an opposite tendency occurs for *Bacteroidia*, *Epsilonproteobacteria*, *Flavobacteriia*, and *Clostridia*, whose abundance increases to 17.52%, 10.14%, 8.25%, and 5.89% from 6.58%, 1.87%, 3.84%, and 4.27%, respectively. However, *Betaproteobacteria* and *Alphaproteobacteria* are still the predominant population, and they are also observed in domestic wastewater, phenol-containing wastewater, and coking wastewater treatment systems. Thus, we consider that they are highly versatile in their ability to degrade contaminants, which is in agreement with Wang et al. [32] and Figuerola et al. [33].

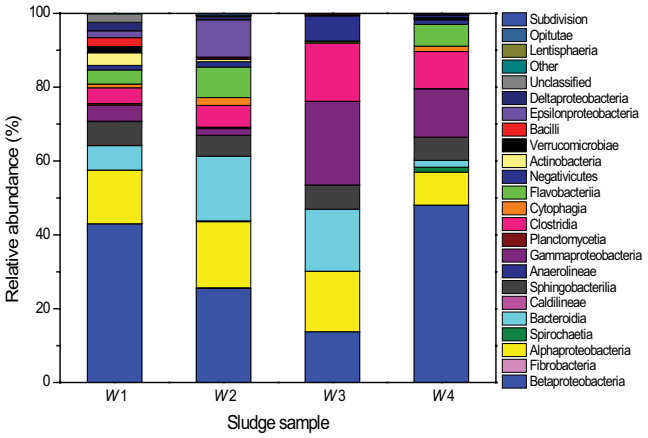

Fig. 9. Class classification level distribution of the bacteria from different periods.

When the influent OLR is increased to 2.47 from 1.25 kg COD/m^3 d, the microbial community structure displays obvious changes and *Gammaproteobacteria* is replaced as the most dominant population (22.6%), followed by *Bacteroidia* (16.8%), *Alphaproteobacteria* (16.34%), and *Clostridia* (15.74%) in sample *W*3. Ibarbalz et al. [27] also observed *Gammaproteobacteria* in polymer industry plant wastewater as the dominant population, whereas in the textile and pharmaceutical plant wastewater, they had low abundance. In sample *W*4, *Betaproteobacteria* once again is the dominant bacteria with 48.07%, followed by *Gammaproteobacteria* with 13.08% and *Clostridia* with 10.05%. Furthermore, the study results also show that some bacterial communities in sample *W*1 disappear in samples *W*3 and *W*4, including *Fibrobacteria* and *Caldilineae*. It can be inferred that *Betaproteobacteria*, *Gammaproteobacteria*, and *Clostridia*, which well adapt to high-carbon sources and growth environment, are the main functional bacteria for the degradation of the tomato processing wastewater. In addition, there is a certain succession change between bacteria, some bacteria are decreased much from W3 to W4, such as *Bacteridia* and *Alphaproteobacteria*, and some bacteria are gradually enriched, such as *Betaproteobacteria* and *Flavobacteria*, the specific mechanism needs further research in the future. From the above, we can conclude that the changing microbial populations during the degradation of the pollutants might be caused by the synergistic effect of the coexistence of the different bacterial communities and their competition with each other to become the dominant degrading bacteria.

4. Conclusions

In this work, aerobic granules with highly efficient performance were successfully cultivated during the treatment of tomato paste processing wastewater using the SBR system mode with a complete cycle time of 4 h. The COD was efficiently removed in the reactor at different organic loads (1.25, 2.47, 3.98, 5.02, and 6 kg COD/(m^3 d)), and the average removal rate of COD of 95.53% wasere achievedat . The present study investigated the formation, characteristics, removal of COD, and succession of microbial community structure of the granular sludge, which demonstrated the feasibility of the cultured aerobic granules for the treatment of the seasonal nature of tomato paste processing wastewater and showed that the aerobic granular sludge technology was the preferable reference for engineering applications.

Acknowledgements

This work was supported by the National Natural Science Foundation of China (No. 51668062) and Science and Technology Innovation Projects for Graduate Students in the Xinjiang Uygur Autonomous Region (XJGRI2016066).

References

[1] Y. Li, Q. Lin, S. Zhang, Research on the degree of integration of Xinjiang tomato industry chain, North. Horticult., 17 (2015) 167–170.

[2] S. Sun, J. Lu, Z. Guo, Z. Sheng, P. Cao, A flexible aeration strategy based on the removal of COD and MLSS in treating tomato paste wastewater, Desal. Wat. Treat., 51 (2013) 2109–2115.
[3] T. Shu, K. Su, Z. Wang, W. Wang, Submerged membrane bioreactor for synthetic tomato processing wastewater treatment: membrane foulant and colloidal particles characterization, Desal. Wat. Treat., 80 (2017) 113–120.
[4] W. Li, P. Cao, C. Li, J. Lu, Treatment of organic wastewater from tomato paste processing by coupled aerobic-anaerobic process, J. Chem. Indus. Eng., 57 (2006) 2970–2975.
[5] X. Zhang, W. Wang, W. Peng, R. Wang, G. Ge, Application and research on the treatment for wastewater from the production of tomato paste by using activated sludge, J. Water Resour. Archi. Eng., 6 (2014) 50–53.
[6] S. Deng, L. Wang, H. Su, Role and influence of extracellular polymeric substances on the preparation of aerobic granular sludge, J. Environ. Manage., 173 (2016) 49.
[7] S.J. Sarma, J.H. Tay, A. Chu, Finding knowledge gaps in aerobic granulation technology, Trends Biotechnol., 35 (2016) 66–78.
[8] M. Figueroa, A. Mosquera-Corral, J.L. Campos, R. Méndez, Treatment of saline wastewater in SBR aerobic granular reactors, Water Sci. Technol., 58 (2008) 479–485.
[9] T. Dobbeleers, D. Daens, S. Miele, J. D'Aes, M. Caluwé, L. Geuens, J. Dries, Performance of aerobic nitrite granules treating an anaerobic pre-treated wastewater originating from the potato industry, Bioresour. Technol., 226 (2016) 211–219.
[10] G. Yilmaz, R. Lemaire, J. Keller, Z. Yuan, Simultaneous nitrification, denitrification, and phosphorus removal from nutrient-rich industrial wastewater using granular sludge, Biotechnol. Bioeng., 100 (2010) 529–541.
[11] K.Z. Su, H.Q. Yu, Formation and characterization of aerobic granules in a sequencing batch reactor treating soybean-processing wastewater, Environ. Sci. Technol., 39 (2005) 2818–2827.
[12] L. Zhu, H.Y. Qi, M.L. Lv, Y. Kong, Y.W. Yu, X.Y. Xu, Component analysis of extracellular polymeric substances (EPS) during aerobic sludge granulation using FTIR and 3D-EEM technologies, Bioresour. Technol., 124 (2012) 455–459.
[13] APHA, AWWA, WEF, Standard Methods for the Examination of Water and Wastewater, American Public Health Association, Washington, D.C., 2012.
[14] B. Zhang, Z. Chen, Z. Qiu, M. Jin, Z. Chen, Z. Chen, J. Li, X. Wang, J. Wang, Dynamic and distribution of ammonia-oxidizing bacteria communities during sludge granulation in an anaerobic–aerobic sequencing batch reactor, Water Res., 45 (2011) 6207–6216.
[15] M.Y. Chen, D.J. Lee, J.H. Tay, Distribution of extracellular polymeric substances in aerobic granules, Appl. Microbiol. Biotechnol., 73 (2007) 1463–1469.
[16] D. Zhou, S. Dong, L. Gao, M. Liu, S. Niu, Distribution characteristics of extracellular polymeric substances and cells of aerobic granules cultivated in a continuous-flow airlift reactor, J. Chem. Technol. Biotechnol., 88 (2013) 942–947.
[17] P.N. Tawakoli, A. Al-Ahmad, W. Hoth-Hannig, M. Hannig, C. Hannig, Comparison of different live/dead stainings for detection and quantification of adherent microorganisms in the initial oral biofilm, Clin. Oral Invest., 17 (2013) 841–850.
[18] I.A. Ivanova, S. Kambarev, R.A. Popova, E.G. Naumovska, K.B. Markoska, C.D. Dushkin, Determination of *Pseudomonas putida* live cells with classic cultivation and staining with "live/dead baclight bacterial viability kit", Biotechnol. Biotechnol. Equip., 24 (2010) 567–570.
[19] M. Pronk, M.K.D. Kreuk, B.D. Bruin, P. Kamminga, R. Kleerebezem, M.C.M.V. Loosdrecht, Full scale performance of the aerobic granular sludge process for sewage treatment, Water Res., 84 (2015) 207–217.
[20] E. Isanta, M.E. Suárez-Ojeda, Á.V.d. Río, N. Morales, J. Pérez, J. Carrera, Long term operation of a granular sequencing batch reactor at pilot scale treating a low-strength wastewater, Chem. Eng. J., 198–199 (2012) 163–170.
[21] J. Wagner, D.G. Weissbrodt, V. Manguin, R.D.C. Rh, E. Morgenroth, N. Derlon, Effect of particulate organic substrate on aerobic granulation and operating conditions of sequencing batch reactors, Water Res., 85 (2015) 158–166.
[22] S.S. Moghaddam, M.R.A. Moghaddam, Cultivation of aerobic granules under different pre-anaerobic reaction times in sequencing batch reactors, Sep. Purif. Technol., 142 (2015) 149–154.
[23] M. Caluwé, T. Dobbeleers, J. D'Aes, S. Miele, V. Akkermans, D. Daens, L. Geuens, F. Kiekens, R. Blust, J. Dries, Formation of aerobic granular sludge during the treatment of petrochemical wastewater, Bioresour. Technol., 238 (2017) 559–567.
[24] A.V.D. Río, M. Figueroa, B. Arrojo, A. Mosquera-Corral, J.L. Campos, G. García-Torriello, R. Méndez, Aerobic granular SBR systems applied to the treatment of industrial effluents, J. Environ. Manage., 95 (2012) S88-S92.
[25] S.S. Adav, D.J. Lee, J.H. Tay, Extracellular polymeric substances and structural stability of aerobic granule, Water Res., 42 (2008) 1644–1650.
[26] J. Gao, Q. Zhang, J. Wng, K. Su, Y. Peng, Enhanced aerobic sludge granulation in sequencing batch reactor by granular activated carbon augmentation, J. Basic Sci. Eng., 20 (2012) 345–354.
[27] F.M. Ibarbalz, E.L. Figuerola, L. Erijman, Industrial activated sludge exhibit unique bacterial community composition at high taxonomic ranks, Water Res., 47 (2013) 3854–3864.
[28] A.J. Li, S.F. Yang, X.Y. Li, J.D. Gu, Microbial population dynamics during aerobic sludge granulation at different organic loading rates, Water Res., 42 (2008) 3552–3560.
[29] Q. Ma, Y. Qu, W. Shen, Z. Zhang, J. Wang, Z. Liu, D. Li, H. Li, J. Zhou, Bacterial community compositions of coking wastewater treatment plants in steel industry revealed by Illumina high-throughput sequencing, Bioresour. Technol., 179 (2015) 436–443.
[30] S. Sun, Z. Guo, R. Yang, Z. Sheng, P. Cao, Analysis of microbial diversity in tomato paste wastewater through PCR-DGGE, Biotechnol. Bioprocess Eng., 18 (2013) 111–118.
[31] P. Cao, Y. Tong, J. Yan, L. Duan, Z. Sheng, Industrial application of aerobic strains to the degradation of wastewater from tomato paste processing, Indus. Water Treat., 31 (2011) 82–85.
[32] X. Wang, M. Hu, Y. Xia, X. Wen, K. Ding, Pyrosequencing analysis of bacterial diversity in 14 wastewater treatment systems in China, Appl. Environ. Microbiol., 78 (2012) 7042–7047.
[33] E.L. Figuerola, L. Erijman, Bacterial taxa abundance pattern in an industrial wastewater treatment system determined by the full rRNA cycle approach, Environ. Microbiol., 9 (2007) 1780–1789.